Mass selectivity of dipolar resonant excitation in a linear quadrupole ion trap

ARTICLE *in* RAPID COMMUNICATIONS IN MASS SPECTROMETRY · MARCH 2014

Impact Factor: 2.25 · DOI: 10.1002/rcm.6795 · Source: PubMed

Research Article

Rapid Communications in Mass Spectrometry

Received: 26 September 2013 Revised: 27 November 2013 Accepted: 27 November 2013 Published online in Wiley Online Library

Rapid Commun. Mass Spectrom. **2014**, *28*, 430–438
(wileyonlinelibrary.com) DOI: 10.1002/rcm.6795

Mass selectivity of dipolar resonant excitation in a linear quadrupole ion trap

D. J. Douglas[1]* and N. V. Konenkov[2]

[1]Department of Chemistry, University of British Columbia, 2036 Main Mall, Vancouver, BC, V6T 1Z1, Canada
[2]Physical and Mathematical Department, Ryazan State University, Ryazan, Svoboda 46, 390000, Russia

RATIONALE: For mass analysis, linear quadrupole ion traps operate with dipolar excitation of ions for either axial or radial ejection. There have been comparatively few computer simulations of this process. We introduce a new concept, the excitation contour, $S(q)$, the fraction of the excited ions that reach the trap electrodes when trapped at q values near that corresponding to the excitation frequency.
METHODS: Ion trajectory calculations are used to calculate $S(q)$. Ions are given Gaussian distributions of initial positions in x and y, and thermal initial velocity distributions. To model gas damping, a drag force is added to the equations of motion. The effects of the initial conditions, ejection Mathieu parameter q, scan speed, excitation voltage and collisional damping, are modeled.
RESULTS: We find that, with no buffer gas, the mass resolution is mostly determined by the excitation time and is given by $R \sim \frac{d\beta}{dq} qn$, where $\beta(q)$ determines the oscillation frequency, and n is the number of cycles of the trapping radio frequency during the excitation or ejection time. The highest resolution at a given scan speed is reached with the lowest excitation amplitude that gives ejection. The addition of a buffer gas can increase the mass resolution. The simulation results are in broad agreement with experiments.
CONCLUSIONS: The excitation contour, $S(q)$, introduced here, is a useful tool for studying the ejection process. The excitation strength, excitation time and buffer gas pressure interact in a complex way but, when set properly, a mass resolution $R_{0.5}$ of at least 10,000 can be obtained at a mass-to-charge ratio of 609. Copyright © 2014 John Wiley & Sons, Ltd.

Dipolar resonant excitation of ions with an auxiliary waveform has found effective use for mass-selective excitation and ejection of ions from three-dimensional Paul traps[1] and for axial[2–4] or radial[5] ejection of ions confined in linear quadrupole ion traps.[6] Resonant dipolar ion excitation in a trap was first described theoretically by Fisher in 1959.[7] Considering an ion as a harmonic oscillator with an external dipolar excitation force, he derived an expression for the resolution, R, of the excitation process as $R = \frac{m}{\Delta m} = 0.84\tau/\tau_{Res}$ for excitation at a frequency corresponding to a Mathieu parameter $q = 0.6$. Here τ is the time at which the ion reaches the electrode surface and τ_{res} is the period of an excitation frequency $\tau_{Res} = 2\pi/(\beta/2 * \Omega)$ where β is a stability parameter and Ω is the angular frequency of the main trapping radio-frequency (rf) field. Thus, to resolve ions with masses m and $m+1$, the times τ for the ions should differ by about one period τ_{Res}. No gas damping was included in the calculation.

In 1991 Schwartz *et al.*[8] demonstrated the operation of a three-dimensional (3D) Paul trap with a mass resolution of ca 30,000 (FWHM) at m/z 502. This high resolution was made possible by gas damping and a very low scan speed of 27.8 Th s^{-1}. (The Th (Thomson) is the mass-to-charge ratio of an ion, m/z, with m, mass, measured in Daltons and z, charge, measured in units of the absolute charge of the electron.)

Following this, the theory of high-resolution excitation of ions in a 3D Paul ion trap with dipolar excitation was developed by Goeringer *et al.*[9] Ion motion was described as a damped harmonic oscillator using the effective potential of the ion trap, an approximation normally assumed to be valid for values of the Mathieu parameter q less than 0.4. The initial phases of the excitation, and ion initial velocities and positions, were not included. Nevertheless this model explained most of the experimental observations at the time; resolution decreases at high scan rates with a peak width proportional to the scan speed, and the addition of a collision gas can increase mass resolution. In the model used by Goeringer *et al.*, the frequency resolution was proportional to the mass resolution. This is true with excitation of ions at low q values because the oscillation frequency is linearly proportional to q. They noted that at high q, where the oscillation frequency is a nonlinear function of q, their model underestimated the mass resolution. Goeringer *et al.* also noted that what is seen in ejection are only the ions that have oscillation amplitudes large enough to reach an end cap of the trap, and these ions can show a higher resolution than the frequency profile. However, the resolution of the ejected ions was not calculated.

* *Correspondence to:* D. J. Douglas, Department of Chemistry, University of British Columbia, 2036 Main Mall, Vancouver, BC, V6T 1Z1, Canada.
E-mail: douglas@chem.ubc.ca

Rapid Communications in Mass Spectrometry

Many of the principles of ion excitation in 3D traps apply to two-dimensional (linear) quadrupole ion traps. Londry and Hager[4] showed that, for mass-selective axial ejection, ions must be excited to a minimum oscillation amplitude to be ejected by the fringe field at the exit of the trap. The required oscillation amplitude increases with the distance from the trap exit, to form a "cone of reflection". Ions with oscillation amplitudes above the cone of reflection are ejected; ions with amplitudes less than the cone are reflected back into the trap. With radial ejection from a linear trap, ions must be excited until they reach a slot in an electrode of the trap.[5] Williams *et al*. studied dipole excitation in a linear trap through "frequency response profiles" (FRP),[10] a graph of ejection time vs excitation frequency. The resolution of the FRP is determined by factors such as the ion excitation time, the amplitude of the auxiliary excitation, the Mathieu parameter q at which ions are excited (q_{eject}), the buffer gas pressure and the spatial harmonics of the trap. It has been shown experimentally that with axial ejection and with a reduction of the scan speed to 5 Th/s, a mass resolution of $R_{0.5} = 6000$ at a mass-to-charge ratio of 609 can be reached[2] with a linear trap with round rods. The low scan speed for high resolution requires the excitation amplitude to be decreased to a few mV.[2] A nitrogen buffer gas pressure of a few mTorr increases the mass resolution with dipolar excitation.[9,10]

The work with both 3D traps and linear traps has mostly considered the oscillation amplitude with different excitation frequencies, without directly modeling the ejection process. In this work we describe an alternative approach. We calculate the fraction of the trapped ions that reaches the electrodes when the excitation frequency is kept constant and ions are trapped at q values near that corresponding to the excitation frequency (the "ejection" q, q_{eject}). We call this the "excitation contour" $S(q)$. The variation of $S(q)$ with q for a fixed excitation frequency (fixed q_{eject}) reveals the resolution with ion ejection, because the trapping voltage V_{rf}, for ions of equal charge, is proportional to the ion mass. The contour $S(q)$ is measured directly in experiments: the output signal is measured with changes of trapping q for different excitation times.

The goal of this work is to determine peak shapes with radial or axial ejection from a linear trap, taking into account the initial conditions by means of numerical simulation of ion trajectories with dipolar resonant excitation of the trapped ions. Our approach differs from those described above in several ways. We use complete trajectory calculations, which are valid at any trapping q value, so we are not limited to the effective potential model. We describe an ensemble of ions with distributions of initial positions and velocities, by averaging of ion trajectories. We calculate the effects of the relative phase of the auxiliary and excitation frequencies, and we calculate the resolution only for ions that are ejected from the trap. This allows the resolution to be determined directly from the parameters of ion motion, q and β. The results are generally in accord with previous experimental results with radial and axial ejection from linear traps. Higher scan speeds reduce the resolution, and adding a collision gas can increase the resolution.

EXPERIMENTAL

The equations of motion in the radial plane of a linear rf quadrupole are:[11,12]

$$\frac{d^2x}{d\xi^2} = -[2q\cos(2(\xi - \xi_0))]x \tag{1}$$

$$\frac{d^2y}{d\xi^2} = +[2q\cos(2(\xi - \xi_0))]y \tag{2}$$

$$\text{where } q = \frac{4eV_{rf}}{(m_i/z)\Omega^2 r_0^2} \tag{3}$$

Here q is a Mathieu parameter, $\xi = \Omega t/2$ is the dimensionless time, x and y are transverse Cartesian coordinates, ξ_0 is the initial rf phase, e is the magnitude of the electronic charge, m_i/z is the ion mass-to-charge ratio, V_{rf} and Ω are, respectively, the amplitude zero to peak, pole to ground, and angular frequency of the trapping rf field, and r_0, the field radius of the quadrupole, is the distance from the quadrupole central axis to an electrode.

In the description of ion motion in the quadrupole field with excitation, the dipole potential within the rods and the interaction between the ions and the buffer gas must be considered. With excitation in the x direction, the dipole potential produces an additional force in x on an ion, F_d,[13] given by:

$$F_d = -A_1 e\frac{V_{ex}}{r_0}\cos(\omega t + \varphi_{ex}) \tag{4}$$

where V_{ex} is the amplitude of the excitation, zero to peak, pole to ground, ω is the angular frequency of the auxiliary dipolar voltage, φ_{ex} is a phase term, and A_1 is a normalization factor of the dipole harmonic of the quadrupole rod set. The drag force F_f on an ion from the buffer gas[13] is:

$$F_f = -\frac{3.01\sqrt{2k_B m_g T_g}}{2}\sigma n_g v, \tag{5}$$

where k_B is Boltzmann's constant, m_g is the collision gas mass, σ is the collision cross section of the ion, n_g is the gas number density, T_g is the gas temperature, and v is the ion velocity. Changing to dimensionless variables $\tilde{x} = x/r_0$ and $\tilde{y} = y/r_0$, and adding the forces F_d and F_f to Eqns. (1) and (2), the resulting equations are:

$$\frac{d^2\tilde{x}}{d\xi^2} = -[2q\cos(2(\xi - \xi_0))]\tilde{x} - 2q_{ex}\cos[2v(\xi - \xi_0) + 2\alpha] - \eta\frac{d\tilde{x}}{d\xi} \tag{6}$$

$$\frac{d^2\tilde{y}}{d\xi^2} = +[2q\cos(2(\xi - \xi_0))]\tilde{y} - \eta\frac{d\tilde{y}}{d\xi} \tag{7}$$

$$\text{where } q_{ex} = \frac{2eA_1V_{ex}}{m_i\Omega^2 r_0^2}, v = \frac{\omega}{\Omega}, \eta = \frac{6.02\sqrt{2k_B m_g T_g}}{m_i\Omega}\sigma n_g \tag{8}$$

and α is the phase shift between the dipolar and main trapping voltages. Comparing definitions of the parameters q (Eqn. (3)) and q_{ex} (Eqn. (8)) gives:

$$q_{ex} = \frac{A_1}{2}q\frac{V_{ex}}{V_{RF}} \tag{9}$$

We model a rod set similar to that used in experiments and earlier modeling studies here[14,15] with $r_0 = 4.17$ mm, rod diameters 9.38 mm. With the normalization factor of the quadrupole field equal to 1, $A_1 = 0.798$. For $m_i = 609$ (reserpine ions) trapped at $q = 0.85$ with a frequency $f = \frac{\Omega}{2\pi} = 1.00$ MHz, the rf amplitude is $V_{rf} \cong$ 921 V. When $q = 0.85$, the amplitude V_{ex} and q_{ex} are related by $V_{ex} = 2717.4 q_{ex}$ (volts, V). Here $\nu = \frac{\omega}{\Omega} = \frac{|2k+\beta|}{2}$, $k = 0, \pm1, \pm2, \ldots$, is a dimensionless frequency, where β is the stability parameter, which determines the ion oscillation frequency spectrum, and β is a function of the parameter q.

'MATHEMATICA 8' was used to solve Eqns. (6) and (7) on a computer with an Intel(R) Core(TM) i7-2600 CPU@3.40GHz processor. To integrate Eqns. (6) and (7) up to 5 000 000 steps were used for time intervals as large as ($\xi = 0 - 10{,}000\pi$).

RESULTS AND DISCUSSION

Excitation time n vs q_{ex}

An important characteristic of dipolar excitation is the dependence of the ejection time, n (measured in cycles of the trapping rf voltage), on the excitation parameter q_{ex} or dipolar voltage amplitude V_{ex}. Because ions have different initial conditions, there is not a universal relation between n and q_{ex}. The maximum time available to excite an ion, n, is determined by the scan speed V_m as $n = f/V_m$; so, for $f = 1.00$ MHz and a scan speed $V_m = 1000$ Th/s, $n = 1000$. If ions are ejected from the trap in less than this maximum excitation period, the excitation time is reduced, because, once ejected, the ions no longer experience the trapping or excitation voltages. This scan speed corresponds to the calculation of the peak from one mass because all ions with a given mass experience the maximum possible time of excitation, n. We first consider the case of no damping gas. The method of calculating n at a given q_{ex} is illustrated in Fig. 1. The time n is the time in which the excited ions reach the rods, so that the dimensionless ion oscillation amplitude $\tilde{x} = 1$. The value of n can be determined graphically in Fig. 1 from $\xi(1) = 430$. The time is $n = 430/\pi \cong 137$ rf cycles.

For dipolar excitation, a number of harmonics with frequencies $\nu_k = \frac{\omega}{\Omega} = \left|\frac{2k+\beta}{2}\right|$, where $k = 0, \pm1, \pm2, \ldots$ can be used. Potentially, operation at higher k values may offer higher resolution. The variation of the ejection time n, with q_{ex}, at $q = 0.85$ ($\beta = 0.77295$), is shown in Fig. 2 for the four main harmonics with frequencies $\nu_0, \nu_{-1}, \nu_{+1}$ and ν_{-2}. For Fig. 2 the initial conditions were , $v_{x0} = v_{y0} = 0.016\pi r_0 f$, $x_0 = y_0 = 0.01 r_0$. On a log-log scale the $n(q_{ex})$ give straight lines with a slope of -1. Thus, the function $n(q_{ex})$ has an universal character $n = c/q_{ex}$, where c is a constant which depends on the ejection q (q_{eject}), the excitation frequency ν_k, and the initial conditions: the initial positions x_0, y_0,velocities $v_{x0} = v_{y0}$, initial rf phases ξ_0, and the phase shift α between the rf voltage and the dipolar excitation. (Equivalently $n = c'/V_{ex}$. For the data with excitation at $\nu_0 = \frac{\beta}{2}$ in Fig. 2, $n = 166/V_{ex}$.) The inverse dependence of n on q_{ex} is caused by the linear dependence of the ion oscillation amplitude on time with resonant dipolar excitation of ion motion with no gas damping,[16] because the equation of ion motion is linear. Increasing the ejection time n requires decreasing the dipolar amplitude q_{ex}. With increasing resonant excitation frequency, ν_k, at a given value of q_{ex}, the ejection time n increases. At the resonant frequency ν_0, small values of q_{ex} lead to long excitation times, n. Use of the harmonics with frequencies ν_{+1} and ν_{-2} is limited because, for a given q_{ex}, the dipolar excitation is relatively small (weak) at times up to 10^4 rf cycles (100 Th/s). The data of Fig. 2 may be used to evaluate the dipolar voltage required for a given scan speed with excitation at $q = 0.85$.

The constant c in $n = \frac{C}{q_{ex}}$ depends only on the initial conditions. To calculate the value of c for given initial conditions it is sufficient to integrate the equation of ion motion for only one value of q_{ex}. In practice, it is important to know the effect of the phase shift, α, on the constant c. Figure 3 illustrates the effect of α on c or the excitation time, n, at $q_{ex} = 0.0005$. The oscillations of c are not periodic because the stability parameter β is an irrational number. We conclude that it is desirable to keep the phase shift α constant so that the phase shift does not change the required excitation time, n.

Excitation contour

The mass selectivity of the dipolar excitation depends on the excitation time n. Ions with similar mass-to-charge ratios, excited for a short time, have approximately the same

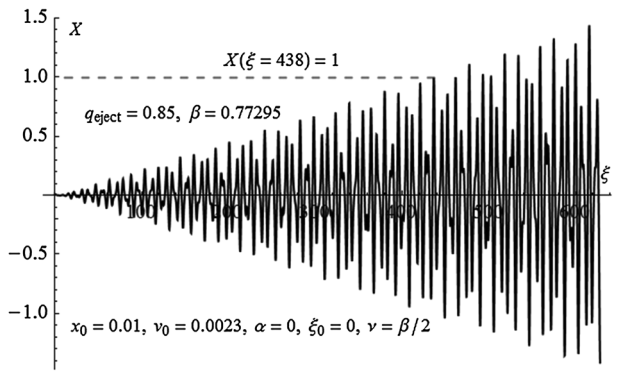

Figure 1. An ion trajectory $x(\xi)$ with dipolar excitation, no gas damping, $q_{ex} = 0.0005$, and the parameters shown.

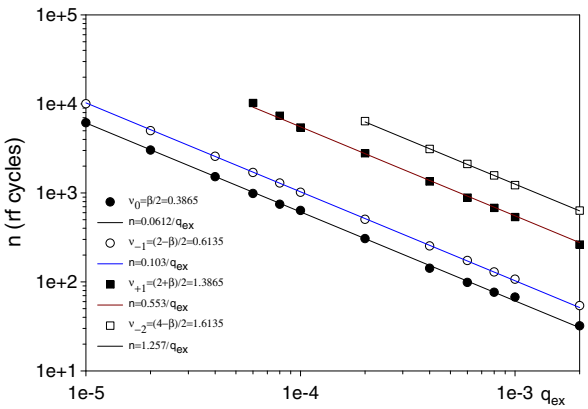

Figure 2. The ejection time n vs q_{ex} for the four harmonics with frequencies $\nu_0, \nu_{-1}, \nu_{+1}$ and ν_{-2}, with $q_{eject} = 0.85$. Initial conditions: , $v_{x0} = v_{y0} = 0.016\pi r_0 f$, $x_0 = y_0 = 0.01 r_0$, $\xi_0 = \alpha = 0$.

Rapid Communications in Mass Spectrometry

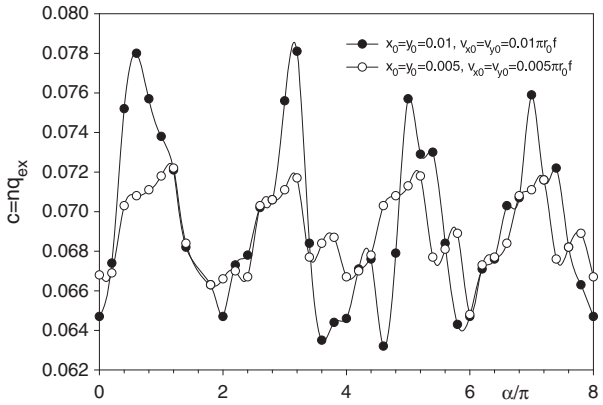

Figure 3. Values of c vs α/π for $q_{ex} = 0.0005$ and different initial conditions. Dipolar excitation: $q_{eject} = 0.85$, $\beta = 0.77295$, $q_{ex} = 0.0005$, $\nu = \beta/2$, $\xi_0 = 0$.

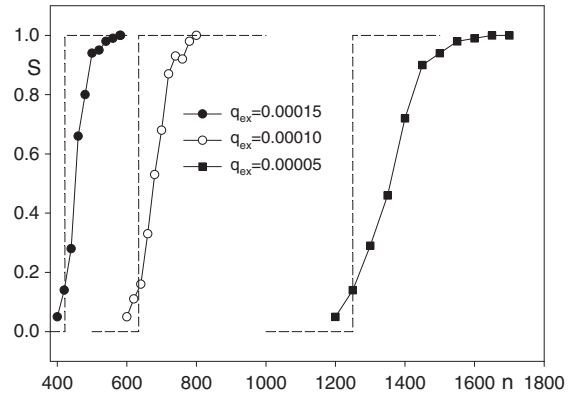

Figure 4. Values of S vs the excitation time, n, for different amplitudes q_{ex}. Dipolar excitation: $q_{eject} = 0.85$, $\nu = \beta/2$. Initial conditions: $\sigma_x = 0.01r_0$, $T = 1000$ K. Dashed lines correspond to excitation with the initial conditions $x_0 = y_0 = 0.01r_0$, $v_{x0} = v_{y0} = 0.016\pi r_0 f$, $\xi_0 = \alpha = 0$.

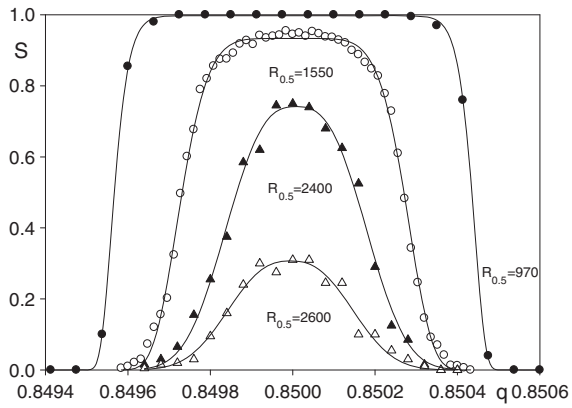

Figure 5. Contours, $S(q)$, with values of q_{ex} of ●, 0.000092; ○, 0.000076; ▲, 0.000070 and Δ, 0.000066, corresponding to V_{ex} = 0.250, 0.207, 0.190 and 0.179 V, respectively. Initial conditions: $\sigma_x = 0.01r_0$, $T = 1000$ K. Excitation at $q_{eject} = 0.85$, $\nu = \beta/2$, $n = 1000$. The solid lines are fits to Eqn. (10).

oscillation spectra and will be detected at the same time. As an integrated characteristic of dipolar excitation of ion collective motion we use a "contour of excitation" (or "excitation peak" "), $S(q) = N_{ex}/N$, where $S(q)$ is the fraction of the ions trapped with Mathieu parameter q which reaches the electrodes in time n, N_{ex} is the number of trajectories of ions, for which $|x(t)| \geq r_0, t \leq n2\pi/\Omega$ and N is the initial number of ion trajectories at a given q with different initial conditions. For this calculation, the emittance of the input ion beam is described by Gaussian distributions of the initial transverse ion positions, thermal initial velocities, and a random uniform distribution of the initial rf phases on the interval [0, π].[17] The initial x, y coordinates are characterized by dispersions $\sigma_x = \sigma_y$ of Gaussian distributions expressed in units of r_0. The initial transverse initial velocities are characterized by thermal distributions with dispersions $\sigma_s \cong 4\times10^{-4}\sqrt{T}$ and are expressed in units of $\pi r_0 f$ (see below) where T is the temperature of ions with mass $m_i = 609$ Da.[17] The main factors which determine the excitation contour $S(q)$ are the excitation time, n, the excitation parameter, q_{ex}, and the pressure of the buffer gas. Typically, 500 trajectories were run to determine a value for $S(q)$.

The line $n(q_{ex})$ in Fig. 2 divides the plane (n,q_{ex}) into two regions where the ion oscillation amplitude $A_x < r_0$ and $A_x > r_0$. Because ions with the same mass have dispersions of initial velocities and positions this line is broadened. This is illustrated in Fig. 4, which shows the curves $S(n)$ for q_{ex} = 0.00015, 0.00010 and 0.00005 for the region where S changes from 0.1 to 1.0. The case of a single fixed initial condition is marked by the dashed lines. The bandwidth Δn, where $0 \leq S \leq 1$, increases with increasing time n. When $S = 1$ all the ions reach the rods. With higher values of n, ions are "over excited". For comparison of excitation contours $S(q)$, we choose the case where $S_{max}(q_0) \cong 0.9$ because in the modeling it is difficult to sustain conditions where $S = 1.00$ (q_0 corresponds to the q value when ions are trapped and excited at the same q to give the maximum number of ejected ions).

Excitation peaks (or excitation contours) $S(q)$ are shown in Fig. 5 for four values of q_{ex}. For all the calculated contours the excitation frequency was fixed at $\nu = 0.3865$ ($q_{eject} = 0.85$) and the trapping q was systematically changed. The procedure for calculating these contours is as follows: at $q = 0.85$, $n = 1000$, and $\nu = \beta/2$, the maximum values of S, S_0, are calculated for an initial value of q_{ex} taken from Fig. 2. Then q_{ex} was systematically changed to find the value that gave $S = 0.90$. By changing the parameter q, the excitation contours $S(q)$ are calculated. Excitation contours with other values of q_{ex} were then calculated. Because the peaks have approximately a symmetrical Gaussian form, the contour $S(q)$ can be described by modified Gaussian curves as:

$$S(q) = S_0 \exp\left[-\frac{1}{2}abs\left(\frac{q - q_0}{b}\right)^m\right] \quad (10)$$

For q_{ex} = 0.000076, for example, S_0 = 0.9335, b = 0.0003, m = 6.0655 and q_0 = 0.85. With decreasing q_{ex}, the mass resolution $R_{0.5}$ is increased from 970 to 2600. The mass selectivity of the dipolar excitation, characterized by $R_{0.5}$, depends strongly on q_{ex} and the excitation time n of an ion. As S increases, the resolution decreases and at higher q_{ex} the ions strike the electrodes more quickly. As a result these ions may be lost in axial or radial ejection. The range of change of the

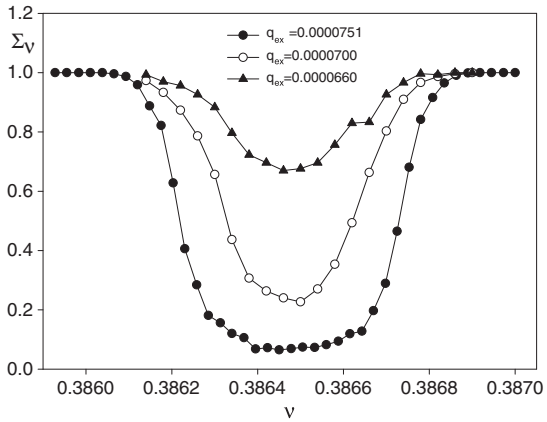

Figure 6. Frequency response curves for $q_{eject} = 0.85$ with $q_{ex} =$ 0.0000751, 0.0000700 and 0.0000660. Excitation time $n = 1000$ rf cycles. Initial conditions: $\sigma_x = 0.01r_0$, $T = 1000$ K.

interconnected parameters n and q_{ex} corresponds to S changing from zero to one. For further comparisons we choose a peak level of 90% ($S_0 = 0.90$).

Frequency response curves, Σ_ν, the fraction of ions remaining in the trap after excitation (Fig. 6), were obtained by changing the auxiliary excitation frequency, $\nu_{ex} = \omega/\Omega$, with the trapping q held constant at $q = 0.85$, for $q_{ex} =$ 0.0000751, 0.0000700 and 0.0000660 ($n = 1000$). The conditions are the same as for Fig. 5. With increasing auxiliary amplitude q_{ex} the frequency resolution $R_{0.5} = \nu_{ex\ 0}/\Delta\nu_{ex}$ measured at one half the peak depth decreases, as in the case of the excitation peaks of Fig. 5. For the auxiliary amplitude q_{ex} =0.000070, the mass resolution $R_{0.5}$ (Fig. 5) exceeds the frequency resolution (Fig. 6) by × 2400/1150 = × 2.1 at $q = 0.85$. The frequency resolution and mass resolution differ because the relation between ν_{ex} and q is nonlinear. Note that $\Sigma_\nu(\nu) \neq 1 - S(q)$ because the functions $\Sigma_\nu(\nu)$ and $S(q)$ have different arguments, ν_{ex} and q.

The effects of the initial conditions, characterized by the parameters σ_x and T, on the excitation contours are illustrated in Fig. 7. The excitation peaks with constant ion temperature $T = 500$ K ($m_i = 609$) and spatial dispersions of Gaussian distributions σ_x = $0.01r_0$, $0.05r_0$, $0.10r_0$ and $0.20r_0$ are shown in Fig. 7(a) for excitation at $q = 0.85$ with the excitation frequency $\nu = \beta/2$. With increasing spatial dispersion, σ_x, the excitation peak $S(q)$ broadens and at $\sigma_x = 0.10r_0$ does not reach the baseline. This is caused by the limited acceptance of the linear trap. With large spatial dispersions some ions are outside the acceptance phase space area and so are ejected from the trap even without excitation. With increases in the ion temperature T from 500 K to 7500 K with a low spatial dispersion, $\sigma_x = 0.01r_0$, the peak broadening is relatively small (Fig. 7(b)).

Mass selectivity

For a given n at $q = 0.85$, the contour $S(q)$ was calculated to find the value of q_{ex} that gives $S(q = 0.85) = 0.90$. Using this peak $S(q)$, the resolution $R_{0.5} = q/\Delta q$ was measured graphically. This modeling of $S(q)$ shows that, at a given q_{eject}, the resolution, R, of an excited ion is proportional to the excitation time n. The variation of $R_{0.5}$ with n is shown in Fig. 8 for ejection at $q_{eject} = 0.80$ and $q_{eject} = 0.85$. The linear increase of the resolution with excitation time n is an important property of dipolar excitation.

The decrease in resolution with decreasing n is related to the finite time of the excitation. A Fourier transform of a finite wave train shows that the frequencies with the largest amplitudes are concentrated in the interval $\Delta\omega = 2\pi/\tau$.[18] Because of the finite time, $\tau = 2\pi n/\Omega$, ions over a mass interval Δm_i are excited. In terms of the dimensionless dipolar frequency $\nu = \omega/\Omega$, the width of the excitation band $\Delta\nu$ can be written as:[15,18]

$$\Delta\nu \lesssim \frac{1}{n} \tag{11}$$

In the range of frequencies $\Delta\nu$, ions with masses m_i in a range Δm_i are subject to resonant excitation. The relation between $\Delta\nu$ and Δm_i can be calculated as follows. At high q the stability parameter β is a nonlinear function of q;[11,12] that is $\beta = \beta(q)$. The increment $\Delta\beta$ of β is related to q by:

$$\Delta\beta = \frac{d\beta}{dq}\Delta q = \beta'(q)q\frac{\Delta q}{q} = \frac{1}{R}\beta'(q)q, \quad R = \frac{q}{\Delta q} = \frac{m_i}{\Delta m_i}. \tag{12}$$

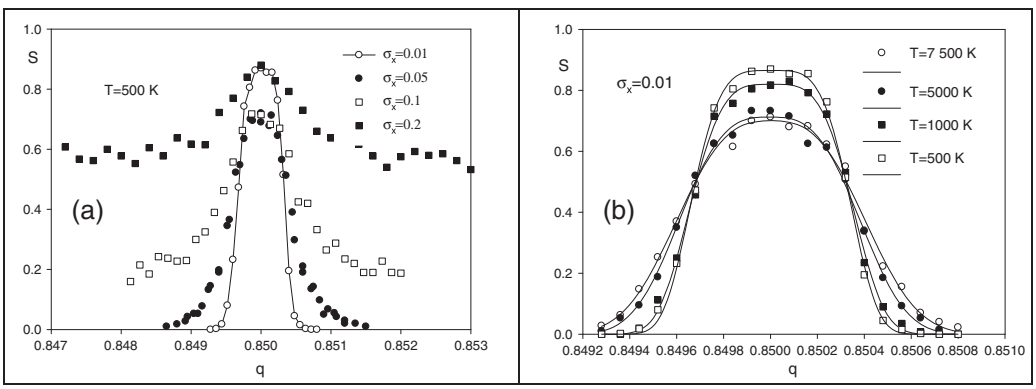

Figure 7. Effects of the initial conditions on the excitation peak shape ($m_i = 609$): (a) spatial dispersions σ_x = $0.01r_0$, $0.05r_0$, $0.10r_0$ and $0.20r_0$ at an ion temperature $T = 500$ K; (b) initial ion temperatures T = 500 K, 1000 K, 5000 K and 7500 K, $m_i = 609$, with a transverse initial position dispersion $\sigma_x = 0.01r_0$. Excitation at $q_{eject} = 0.85$, excitation frequency $\nu = \beta/2$.

Rapid Communications in Mass Spectrometry

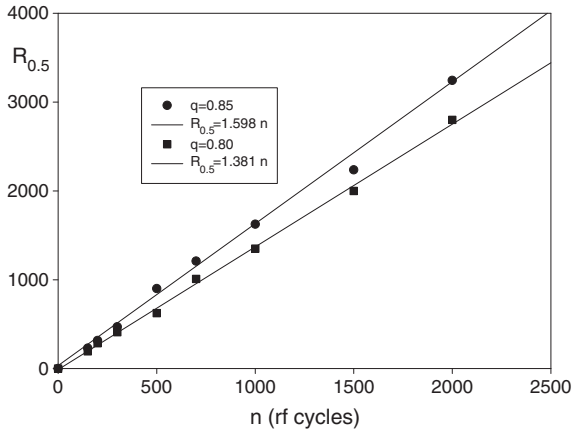

Figure 8. Selectivity of ion excitation, $R_{0.5}$, vs excitation time, n, for ions with $m_i = 609$. Initial conditions: $\sigma_x = 0.01 r_0$, $T = 1000$ K. Dipolar excitation: $q_{eject} = 0.85$, $\nu = \beta/2$, $R = q/\Delta q$. The selectivity, $R_{0.5}$, of the dipolar excitation was determined from the excitation contours $S(q)$ at the 50% level.

Because $\nu = \frac{\beta}{2}$ and $\Delta\nu = \Delta\beta/2$ we find that the resolution, R, with dipolar excitation is given by:

$$R = \frac{1}{2}\beta'(q)qn \tag{13}$$

where $\beta' = d\beta/dq$.

Figure 9 shows peaks for excitation frequencies $\nu = \beta/2$, $\nu = \beta/2 + 1/2n$ and $\nu = \beta/2 + 1/n$ with $n = 1000$. According to the Rayleigh criterion,[19] two excitation contours $S(q)$ are distinguished if they overlap at the half-height of the peaks. In Fig. 9 this occurs when the frequency interval $\Delta\nu$ is $1/2n$. For the resolution $R_{0.5}$, which is determined for one half of the excitation contour height, we find from Eqns. (12) and (13) that:

$$\frac{2}{2n} = \frac{1}{R_{0.5}}\beta'(q)q \text{ and } R_{0.5} = 2R \cong \beta'(q)qn \tag{14}$$

The function $\beta'(q)q$ vs q is shown in Fig. 10. Figure 10 also shows the variation of $R_{0.5}\frac{1}{n}$ as a function of q for the two excitation frequencies, ν_0 and ν_{-1}. The resolution values

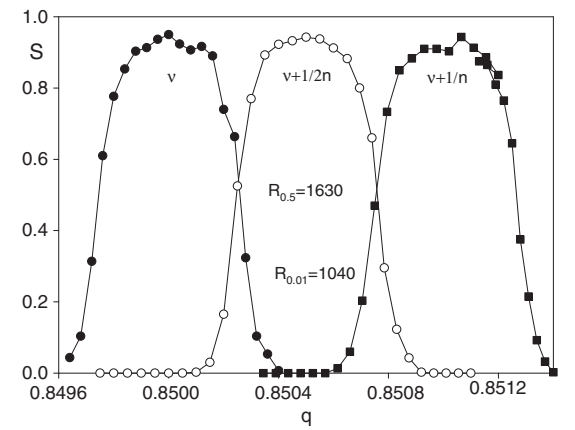

Figure 9. Mass selective curves for different excitation frequencies $\nu = \beta/2$, $\nu = \beta/2 + 1/2n$, and $\nu = \beta/2 + 1/n$, for $q = 0.85$, $n = 1000$ rf cycles, $q_{ex} = 0.000076$. Initial conditions: $\sigma_x = 0.01 r_0$, $T = 1000$ K.

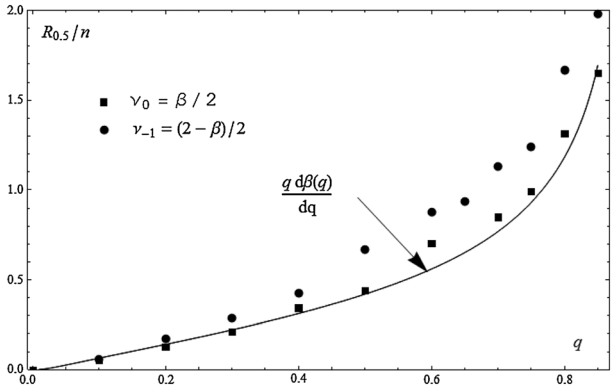

Figure 10. Resolution $R_{0.5}$ as a function of q_{eject} for $n = 1000$ rf cycles (marked by the points) for the two main harmonics with frequencies ν_0 and ν_{-1}, and the theoretical curve $\beta'(q)q$ as a function of q. Initial conditions: $\sigma_x = 0.01 r_0$, $T = 1000$ K.

$R_{0.5}$ were determined from excitation contours for $n = 1000$. A similar formula for the resolution was derived for the case where $\beta \sim q$ by Collings *et al.*[20] Using Eqn. (14) we can relate the resolution $R_{0.5}$ to the scan speed V_m as:

$$R_{0.5} = \beta'(q)qf/V_m \tag{15}$$

From Eqn. (15) it follows that the resolution $R_{0.5}$ is proportional to the trapping frequency $f = 2\pi/\Omega$ and inversely proportional to the scan speed V_m.

The dispersion and deviation of the calculated points from the curve may be caused by difficulties in maintaining the level of excitation at $S_0 = 0.90$ in the numerical modeling, and also the definition of the value of $R_{0.5}$. The mass resolution is slightly greater with excitation at ν_{-1}. The main result is that the calculated points follow the theoretical curve $R \sim \beta'(q)qn$. This means that Eqn. (15) is valid for dipolar excitation and confirms the mechanism of the peak broadening proposed by Fisher. A contour $S(q)$ is calculated for ions of one mass, but having various initial conditions in the quadrupole field. Although the initial conditions can contribute to peak broadening, this broadening is caused mainly by the finite excitation time. The highest resolution requires excitation at higher q values. However, the quadrupole acceptance decreases as q approaches the stability boundary at $q = 0.908$, decreasing the sensitivity.

The required excitation amplitudes, q_{ex}, for the excitation frequencies ν_0 and ν_{-1} vs q_{eject} for the conditions of Fig. 10 are shown in Fig. 11. The two curves $q_{ex}(q_{eject})$ differ significantly; for the frequency ν_{-1}, the required amplitude q_{ex} decreases continuously with q_{eject}, whereas, with excitation at ν_0, the amplitude passes through a maximum near $q_{eject} = 0.7$.

In the Sudakov effective potential model for high q, the well depth decreases with increasing q.[21] For resonant removal of an ion from a trap in a given time, n, the amplitude q_{ex} of dipolar excitation has to be proportional to the depth of the potential well. Gao and Douglas[22] recently found that at high q the well depth of the effective potential and the oscillation frequency are better described by the standard effective potential model with a well depth D given by $D = qV_{rf}/4$.[23] This well depth increases continually up to

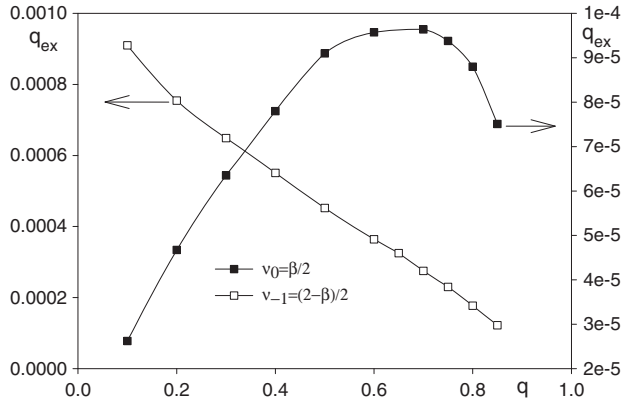

Figure 11. Required excitation amplitude q_{ex} vs q_{eject} for an ejection time $n = 1000$ and for the two resonant frequencies ν_0 and ν_{-1}. Initial conditions: $\sigma_x = 0.01 r_0$, $T = 1000$ K.

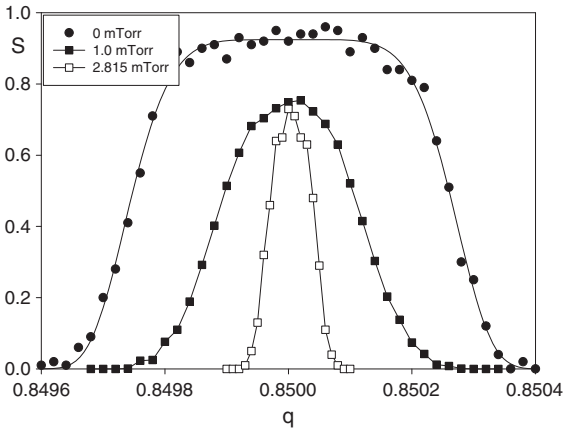

Figure 12. Excitation contours for buffer gas pressures of 0.0, 1.000 and 2.815 mTorr with $R_{0.5}$ of 1,625, 2,830 and 10,000, respectively, and $q_{ex} = 0.000075$ (0.0 mTorr) or 0.00030 (1.000 and 2.815 mTorr). Excitation at $q_{eject} = 0.85$, excitation frequency $\nu_0 = \beta/2 = 0.386475$, excitation time $n = 1000$. The solid lines are fits to Eqn. (10). Initial conditions $\sigma_x = 0.01 r_0$, $T = 1000$ K.

the stability boundary limit at $q = 0.908$, suggesting that the required excitation amplitude should also increase continuously with q.

The decrease in required excitation amplitude at high q_{eject} may be related to the acceptance of the quadrupole which decreases to zero at $q = 0.908$. Excited ions need not reach r_0 to become unstable in the quadrupole field. If they are outside the acceptance at $r < r_0$, they will still be ejected, so that smaller values of q_{ex} can lead to ejection in the same time ($n = 1000$ in Fig. 11). In fact the curve of q_{ex} vs q for ν_0 in Fig. 11 is qualitatively like the acceptance of a linear rf-only quadrupole in one dimension (say x) calculated by Dawson and Fulford.[24] However, this does not explain the behavior with excitation at ν_{-1}.

Every point in Fig. 11 corresponds to a point in Fig. 10 with a defined resolution $R_{0.5}$ and with an excitation time $n = 1000$. These plots of $q_{ex}(q)$ allow the excitation amplitude q_{ex} required when $n = 1000$ to be evaluated. At the same time the plot of $R_{0.5}$ as a function of q in Fig. 10 is applicable to any excitation The decrease in required excitation amplitude at high q_{eject} may be related to the q_{eject} and any excitation time n, but it is necessary to find the excitation amplitude q_{ex}.

Effects of gas damping

Buffer gas in a linear trap leads to damping of the ion motion. This changes the excitation contour $S(q)$. The description of the ion motion in a buffer gas used the drag force described by Eqn. (5). Protonated reserpine ions ($m_i = 609$, collision cross section 280 Å^2[25]) and a N_2 buffer gas with pressures 1–3 mTorr were modeled.

Adding a buffer gas leads to increases in the resolution of mass-selective ejection with dipolar excitation. This is illustrated in Fig. 12 which shows excitation contours, $S(q)$, for ions of $m_i = 609$ and N_2 pressures of 0.000, 1.000 and 2.815 mTorr. At 2.815 mTorr a resolution $R_{0.5} = 10,000$ is achieved, increased from $R_{0.5} = 1,625$ at zero pressure (scan speed 1000 Th/s, ($n = 1000$)). Introduction of dissipative losses through collisions of ions with molecules of a buffer gas in an oscillatory system has to lead to a decrease in the quality factor (Q) and therefore to decreases in the resolution of the excitation resonance. However, as noted, it is only the ions that reach $x = r_0$ that contribute to $S(q)$. Even if the excitation resonance is broadened, the range of frequencies over which ions reach r_0 can be decreased.

Narrowing of a mass-selective peak $S(q)$ may partly be due to collisional cooling of ions. With collisional cooling, there is a loss of memory of the initial conditions and the initial spatial and energy spreads are reduced. The energy relaxation time is $1/4\lambda$ where is λ is given by:[13]

$$\lambda = \frac{3.01\sqrt{2k_B m_g T_g}}{4m_i}\sigma n_g \qquad (16)$$

At 1.000 mTorr the energy relaxation time is calculated to be 1.87×10^{-4} s ($n = 187$) and at 2.815mTorr, 6.64×10^{-5} s ($n = 66.4$). The greater resolution at 2.815 mTorr may in part be due to greater collisional cooling at this higher pressure. With increasing buffer gas pressure the required dipolar amplitude, q_{ex}, increases by × 4, from 7.5×10^{-5} (0.204 V) to 3×10^{-4} (0.815 V).

The dependencies of peak heights S_0 on the pressure, p, of the buffer gas N_2 are shown in Fig. 13. There are narrow bands of pressure for a given q_{ex} where the value of S_0 changes from 0 to 1. The curve $S_0(p)$ divides the region (or plane) (S_0, p); to the left, ions are ejected or strike the rods, and to the right ions are not ejected. Increasing the pressure causes the curves to shift to higher values of q_{ex}, and the width of the band, Δp, to decrease. To locate these bands, the pressures, p, vs q_{ex} at which $S(q_{ex}) = S_0/2$ were determined. This dependence $p(q_{ex})$ is shown in Fig. 14. With increasing p, the required amplitude q_{ex} increases approximately linearly. Along this curve, $p(q_{ex})$, there is a narrow band where the value of S_0 changes between 0 and 1. The resolution can be adjusted within this band. This band divides the plane (p,q_{ex}) into two regions, where $S_0 = 0$ (no ejection of ions) and $S_0 = 1$ (q_{ex} equal to or greater than required to eject all ions).

Contours with $R_{0.5} = 10,000$ and 31,480 at a pressure of 2.815 mTorr for excitation times $n = 1000$ and 2000 rf cycles are shown in Fig. 15 for the second resonant

Rapid Communications in Mass Spectrometry

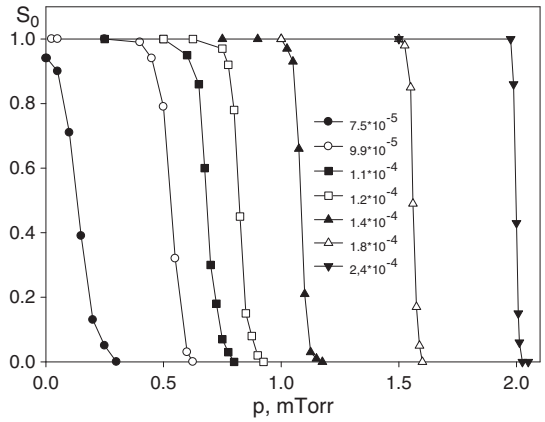

Figure 13. The selectivity S_0 (max $S(q)$) vs buffer gas pressure p (N_2) for ions with $q_{eject} = 0.85$, $v = \beta/2$, $m_i = 609$, $n = 1000$. Initial conditions, $\sigma_x = 0.01 r_0$, $T = 1000$ K. Each curve has a different value of q_{ex}.

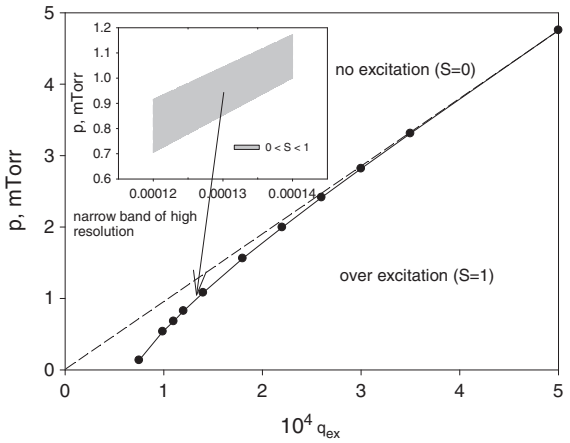

Figure 14. The relation between the buffer gas (N_2) pressure and q_{ex} determined with $S(q_{ex}) = S_0/2$. The dashed line is the asymptotic line p [mTorr] = $9510 q_{ex}$. With $\sigma_x = 0.01 r_0$, $T = 1000$ K, $q_{eject} = 0.85$, $v = \beta/2$, $n = 1000$.

frequency $v_{-1} = (2 - \beta)/2$ with excitation at $q_{eject} = 0.85$. Doubling the excitation time n approximately triples the resolution. With a damping gas the resolution is no longer described by the simple relation of Eqn. (15). A given resolution at excitation frequency v_{-1} might be achieved with a decreased excitation time.

Achieving a resolution $R_{0.5} = 30,000$ requires stability and reproducibility of the amplitude of the dipolar potential of $1/4997 = 0.0002$ or 0.02% or better. The same stability and reproducibility are required for the gas pressure. A change of q of only 0.00002 leads to $S = 1$ or $S = 0$. Achieving resolution as high as this using gas damping requires careful experiments.

CONCLUSIONS

In this work, we introduced the concept of the excitation contour, $S(q)$, of dipolar excitation in a linear quadrupole. The excitation contour is calculated with numerical

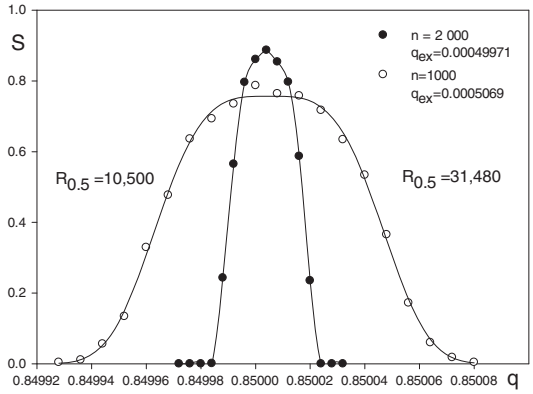

Figure 15. Peaks $S(q)$ at a buffer gas pressure of 2.815 mTorr for excitation times of 1000 and 2000 rf cycles. Resonant frequency $v_{-1} = (2 - \beta)/2$.

simulations, and shows that, with no collisional damping, the broadening of the mass peak is mainly related to the excitation time, which is controlled by the scan speed. As a result, the resolution is proportional to the excitation time, n. With increasing q_{eject}, the resolution increases, determined by the function $q\beta'(q)$. The two excitation frequencies v_0 and v_{-1} give approximately the same resolution. With no damping gas, the time of the excitation, n, and the amplitude of the dipolar excitation, q_{ex}, are strongly coupled as $q_{ex} \sim 1/n$ or $V_{ex} \sim f/V_m$. To obtain the highest resolution with $S_0 \leq 1$ at a low scan speed, say 20 Th/s ($n = 5000$ for $f = 1.0$ MHz), the excitation amplitude should be low, about 30 mV for the quadrupole modeled here. Adding a drag force to the equations of ion motion shows that a buffer gas increases the resolution by up to factor of 6 (e.g. from 1,625 to 10,000 in Fig. 12). The three parameters, excitation time n, excitation strength q_{ex}, and buffer gas pressure p, are related in a complex way but, when set properly, a resolution of at least $R_{0.5} = 10,000$ can be obtained at m/z 609.

The process of mass-selective axial ejection for ion detection[2–4] is not included in detail in these simulations. However, the simulations do include the key step of exciting ions to large oscillation amplitudes. Because these simulations require that ions reach an electrode for ejection, they might most suitably be applied to radial ejection through a trapping electrode. Nevertheless the simulations are in qualitative agreement with experimental observations for both radial and axial ejection from linear traps; at low scan speeds the dipolar voltage should be small and the resolution is highest,[2–4] the resolution is greater with excitation at $q = 0.85$ than at lower q,[2,4,5,20] and a low pressure buffer gas can increase the mass resolution.[9,10] In future we would like to extend this work to study the effects of space charge on $S(q)$. It would also be of interest to apply this method to distorted quadrupole fields that contain higher multipoles.

Acknowledgements

Supported by the Natural Sciences and Engineering Research Council of Canada and AB Sciex through an Industrial Research Chair.

REFERENCES

[1] R. E. March. Quadrupole ion traps. *Mass Spectrom. Rev.* **2009**, *28*, 961.
[2] J. W. Hager. A new linear ion trap mass spectrometer. *Rapid Commun. Mass Spectrom.* **2002**, *16*, 512.
[3] J. W. Hager. Performance optimization and fringing field modifications of a 24-mm long rf-only quadrupole mass spectrometer. *Rapid Commun. Mass Spectrom.* **1999**, *13*, 740.
[4] F. A. Londry, J. W. Hager. Mass selective axial ion ejection from a linear quadrupole ion trap. *J. Am. Soc. Mass Spectrom.* **2003**, *14*, 1130.
[5] J. C. Schwartz, M. W. Senko, J. E. P. Syka. A two-dimensional quadrupole ion trap mass spectrometer. *J. Am. Soc. Mass Spectrom.* **2002**, *13*, 659.
[6] D. J. Douglas, A. J. Frank, D. Mao. Linear ion traps in mass spectrometry. *Mass Spectrom. Rev.* **2005**, *24*, 1.
[7] E. Fischer. Die dreidimensionale stabilisierung von ladungsträgern in einem vierpolfeld. *Zeitschrift fur Physik* **1959**, *156*, 1.
[8] J. C. Schwartz, J. E. P. Syka, I. Jardine. High resolution on a quadrupole ion trap mass spectrometer. *J. Am. Soc. Mass Spectrom.* **1991**, *2*, 198.
[9] D. E. Goeringer, W. B. Whitten, J. M. Ramsey, S. A. McLuckey, G. L. Glish. Theory of high-resolution mass spectrometry achieved via resonance ejection in the quadrupole ion trap. *Anal. Chem.* **1992**, *64*, 1434.
[10] S. M. Williams, K. W. M. Siu, F. A. Londry, V. I. Baranov. Resonant excitation by linear ion trap simulations. *J. Am. Soc. Mass Spectrom.* **2007**, *18*, 578.
[11] R. E. March, R. J. Hughes. *Quadrupole Storage Mass Spectrometry.* John Wiley & Sons, New York, **1989**, p. 44.
[12] P. H. Dawson, in *Quadrupole Mass Spectrometry and Its Applications*, (Ed: P. H. Dawson). AIP Press, Woodbury, **1995**, pp. 13–15.
[13] A. L. Michaud, A. J. Frank, C. Ding, X. Zhao, D. J. Douglas. Ion excitation in a linear quadrupole ion trap with an added octopole field. *J. Am. Soc. Mass Spectrom.* **2005**, *16*, 835.
[14] H. Qiao, C. Gao, D. Mao, N. Konenkov, D. J. Douglas. Space charge effects with mass selective axial ejection from a linear quadrupole ion trap. *Rapid Commun. Mass Spectrom.* **2011**, *25*, 3509.
[15] D. J. Douglas, N. V. Konenkov. Trajectory calculations of space-charge-induced mass shifts in a linear quadrupole ion trap. *Rapid Commun. Mass Spectrom.* **2012**, *26*, 2105.
[16] W. Xu, W. Chappell, Z. Ouyang. Modeling of ion transient response to dipolar AC excitation in a quadrupole ion trap. *Int. J. Mass Spectrom.* **2011**, *308*, 49.
[17] N. Konenkov, F. Londry, C.-F. Ding, D. J. Douglas. Linear quadrupoles with added hexapole fields. *J. Am. Soc. Mass Spectrom.* **2006**, *17*, 1063.
[18] G. Arfken. *Mathematical Methods for Physicists*. Academic Press, New York, **1968**, p. 529.
[19] F. A. Jenkins, H. E. White. *Fundamentals of Optics*, (3rd edn.). McGraw-Hill Book Company Inc., New York, **1957**, p. 300.
[20] B. A. Collings, W. R. Stott, F. A. Londry. Resonant excitation in a low pressure linear ion trap. *J. Am. Soc. Mass Spectrom.* **2003**, *14*, 622.
[21] M. Sudakov. Effective potential and the ion axial beat motion near the boundary of the first stable region in a nonlinear ion trap. *Int. J. Mass Spectrom.* **2001**, *206*, 27.
[22] C. Gao, D. J. Douglas. Can the effective potential of a linear quadrupole be extended to values of the Mathieu parameter *q* up to 0.90? *J. Am. Soc. Mass Spectrom.* **2013**, *24*, 1848.
[23] D. Gerlich. Inhomogeneous rf fields: A versatile tool for the study of processes with slow ions. *Adv. Chem. Phys.* **1992**, *LXXXII*, 1.
[24] P. H. Dawson, J. E. Fulford. The effective containment of parent ions and daughter ions in a triple quadrupole used for collisional dissociation. *Int. J. Mass Spectrom. Ion Phys.* **1982**, *42*, 195.
[25] G. Javahery, B. A. Thomson. A segmented radiofrequency-only quadrupole collision cell for measurements of ion collision cross section on a triple quadrupole mass spectrometer. *J. Am. Soc. Mass. Spectrom.* **1997**, *8*, 697.

